Appendix G
DYNAMIC SOIL-STRUCTURE INTERACTION ANALYSIS OF KENTUCKY LOCK WALL

G-1. Background

Kentucky Lock is located in western Kentucky at Mile 22.4 on the Tennessee River. In order to reduce shipping delays of the Tennessee and Cumberland River systems, a new 33.53-m wide by 365.76-m long (110 ft x 1200 ft) navigation lock is being constructed landward and adjacent to the existing 33.53-m wide by 182.88-m long (110 ft x 600 ft) lock (Figure G-1). The project was authorized in 1996 and construction commenced in 1998. In this example, Culvert Valve Monolith L4 of the lock addition is considered for the soil-structure-interaction (SSI) analysis. Figure G-2 shows general dimensions and geometry of this monolith.

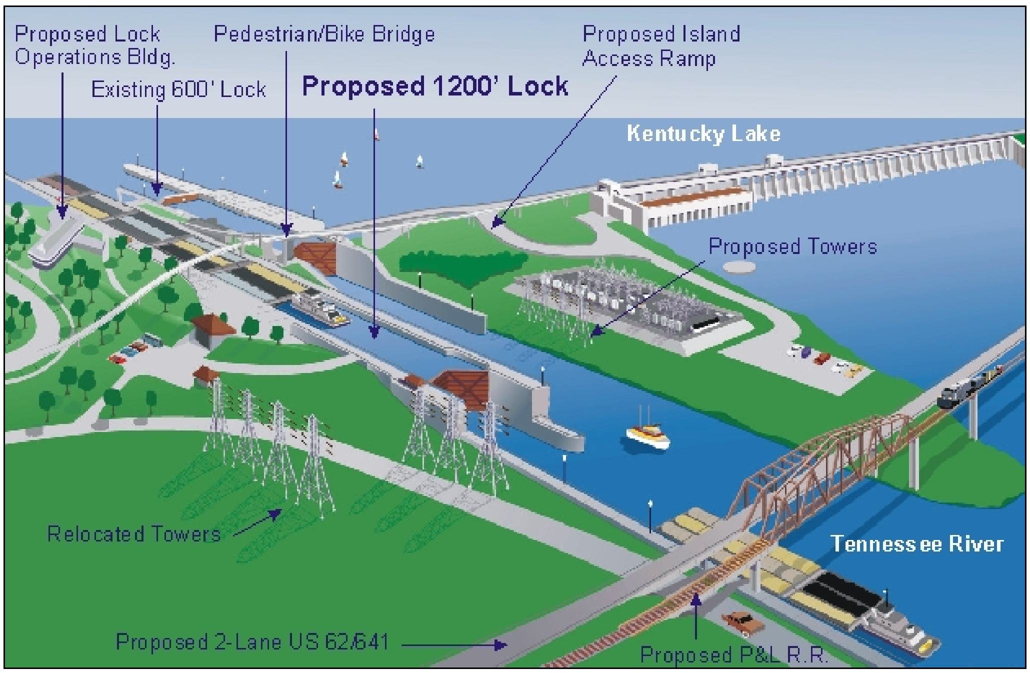

Figure G-1. Kentucky Lock Addition Project

G-2. Purpose and Objectives

The purpose of this example is to demonstrate an approach used to perform dynamic SSI analysis for the proposed Kentucky Lock Addition using time-history analysis. The objectives of the analysis are:

a. To assess dynamic sliding stability at different sections of the monolith

b. To compute dynamic backfill soil pressure at the time of peak response

c. To study nonlinearity of backfill material during dynamic loading

G-3. Scope

The scope of the study included the following:

a. Definition of acceleration time histories for design ground motion

b. Estimation of dynamic properties of backfill material and site rock profiles

c. Development of finite-element model for lock wall-backfill soil system

d. Analysis for dynamic loading

e. Evaluation of response of concrete monolith and backfill soil for earthquake loading

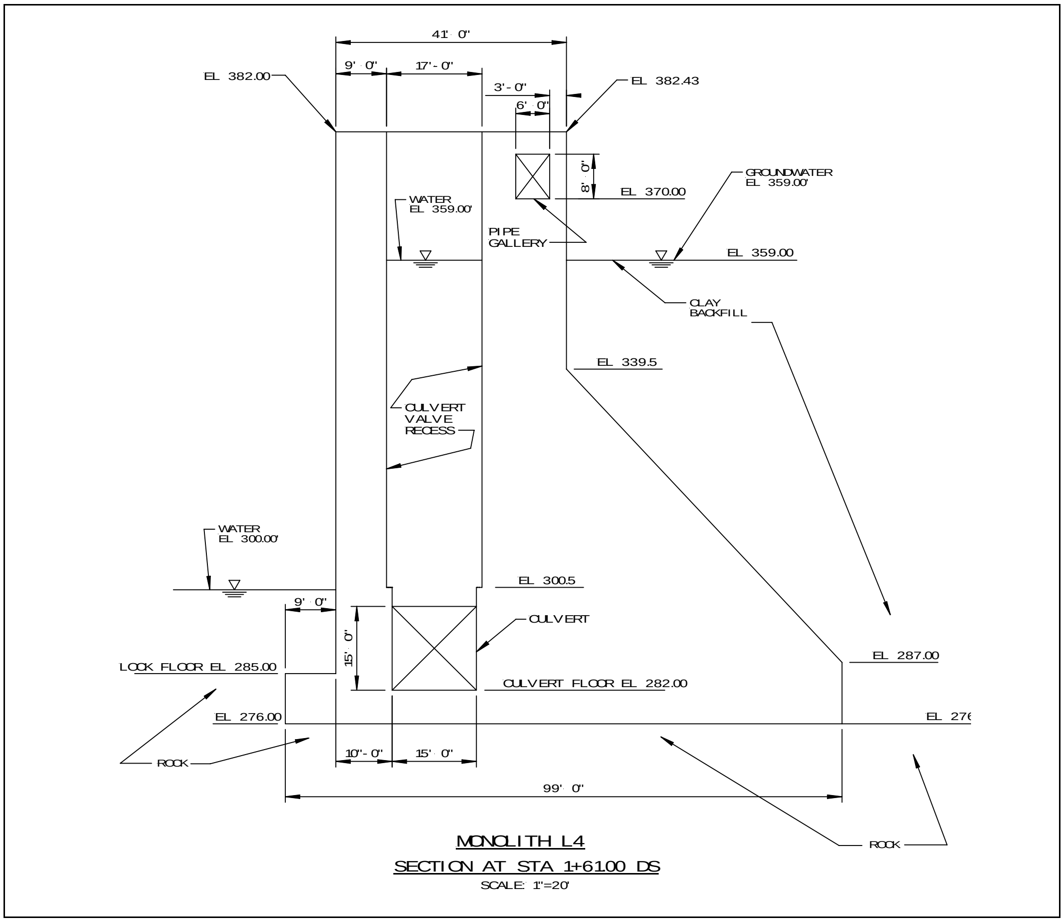

Figure G-2. General dimensions and geometry of Culvert Valve Monolith L4

G-4. Method of Analysis

a. Dynamic SSI analysis can be performed using finite-element method. The soil-structure continuum consisting of the lock monolith, foundation rock and backfill soil is modeled using 2-D plane strain elements. Using this approach, dynamic inertia interaction and wave propagation phenomenon are considered directly.

b. Computer program QFLUSH (Quest Structures 2001), an enhanced version of FLUSH (Lysmer et al. 1975) with pre- and post-processing capabilities, was used to study dynamic SSI analysis of Kentucky Lock monolith. The analyses were performed in the frequency domain for vertically propagating shear and compression waves (from horizontal and vertical excitations). Responses from horizontal and vertical excitations were obtained separately and then combined. The nonlinear soil behavior was approximated by the equivalent linear techniques through iterative procedures. The results for the horizontal and vertical excitations were transformed from the frequency domain back to the time domain. The time-domain results were subsequently combined to obtain the total response for simultaneous horizontal and vertical (shear- and compression- wave) excitations.

G-5. Finite Element Modeling

a. Finite-element Mesh. The Kentucky Culvert Valve Monolith L4 is founded on rock and backfilled by sand on the land side. An idealized stratigraphic profile of the foundation and backfill soil with the lock wall section is shown in Figure G-3. The lock wall, foundation rock, and the backfill soil were modeled by plane-strain 2-D quadrilateral elements with concrete, rock, and soil material properties, respectively. The finite element representation of the lock wall, foundation rock, and the backfill is shown in Figure G-4. The model consisted of 1,693 plane-strain elements. The effect of culvert recess was simulated by smearing the mass and stiffness properties of the region with the recess over a similar region without the recess. This was done by proportioning the mass and stiffness properties according to the volume ratio of the region with and without the recess.

b. Boundary Conditions and Element Size. The model was extended approximately one lock height to the right and one lock height to the left. The bottom boundary was placed at approximately 15.24 m (50 ft) below the lock base. Transmitting boundaries were established at the right and left sides of the model and rigid boundary was assumed at the bottom of the model. Transmitting boundary was used to minimize the horizontal extent of the model and ensure that seismic waves propagating away from the structure are absorbed by the boundary and not reflected back. However, the boundaries were placed far enough from the lock wall so that accurate representations of dynamic interaction effects between the structure and backfill soil and between the structure and foundation rock can be achieved. The element heights were selected using the equation below given in the FLUSH manual such that frequencies up to 30 Hz could be included in the analysis.

$$h_{\max} = \frac{1}{5} \cdot \frac{V_s}{f_{\max}}$$

In this equation V_s is the lowest shear wave velocity reached during iterations and f_{max} is the highest frequency of the analysis. Although there is no restriction of element dimension in horizontal direction in QFLUSH, relatively short elements were used to improve accuracy of analyses.

c. Added Hydrodynamic Mass. The hydrodynamic effects of water on the lock wall were considered by the Westergaard's added mass solution (EM 1110-2-6051). The added mass coefficients were effective only in the direction perpendicular to the lock wall. The water inside the culvert valve recess is fully constrained. The added hydrodynamic mass for the inside water was therefore taken equal to the mass of water. The added mass for each node was computed according to its tributary area.

G-6. Material Parameters

a. Basic Material Properties. Uniform properties were assumed for the backfill soil and the foundation rock. It was considered that engineered backfill will be used. The basic material properties for the concrete, foundation rock, and the backfill sill are listed in Tables G-1 to G-3.

Table G-1

Concrete Properties	English Units		Metric Units	
Unit weight (γ_s)	145	pcf	2,322.68	Kg/m^3
Compressive strength	3,000	psi	20.68	MPa
Poisson's ratio (estimated)	0.20		0.20	
Elastic modulus (estimated)	3×10^6	psi	20,684.27	MPa
Shear modulus	1.25×10^6	psi	8,618.45	MPa
Shear wave velocity	6,322	fps	1,926.95	m/s

Table G-2

Rock Properties	English Units		Metric Units	
Unit weight ( )	166.6	pcf	2668.68	Kg/m^3
Peak friction angle ( )	36.7	degrees	36.7	degrees
Cohesion (c)	13.2	psi	91.01	KPa
Unconfined compressive strength	28,296	psi	195.09	MPa
Poisson's ratio	0.3		0.3	
Elastic modulus	5.51×10^6	psi	37,990.11	MPa
Shear modulus	2.119×10^6	psi	1,4610.00	MPa
Shear wave velocity	7,680	fps	2,340.86	m/s

Table G-3

Granular Backfill Properties	English Units		Metric Units	
Saturated unit weight (γ_s)	135	pcf	2,162.49	Kg/m^3
Peak friction angle (ϕ)	32	degrees	32	degrees
Cohesion (c)	0	psf	0	MPa
Poisson's ratio (estimated)	0.30		0.3	
Elastic modulus (estimated)	13.187×10^6	psf	631.40	MPa
Shear modulus	5.072×10^6	psf	242.85	MPa
Shear wave velocity	1,100	fps	335.28	m/s

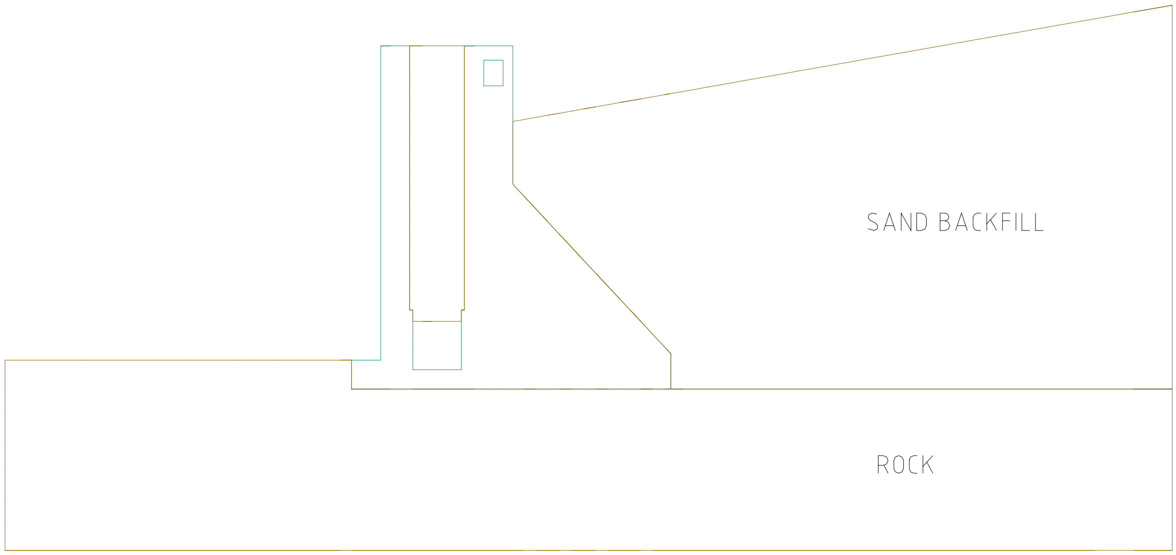

Figure G-3. Idealized stratigraphic profile at the Kentucky lock site

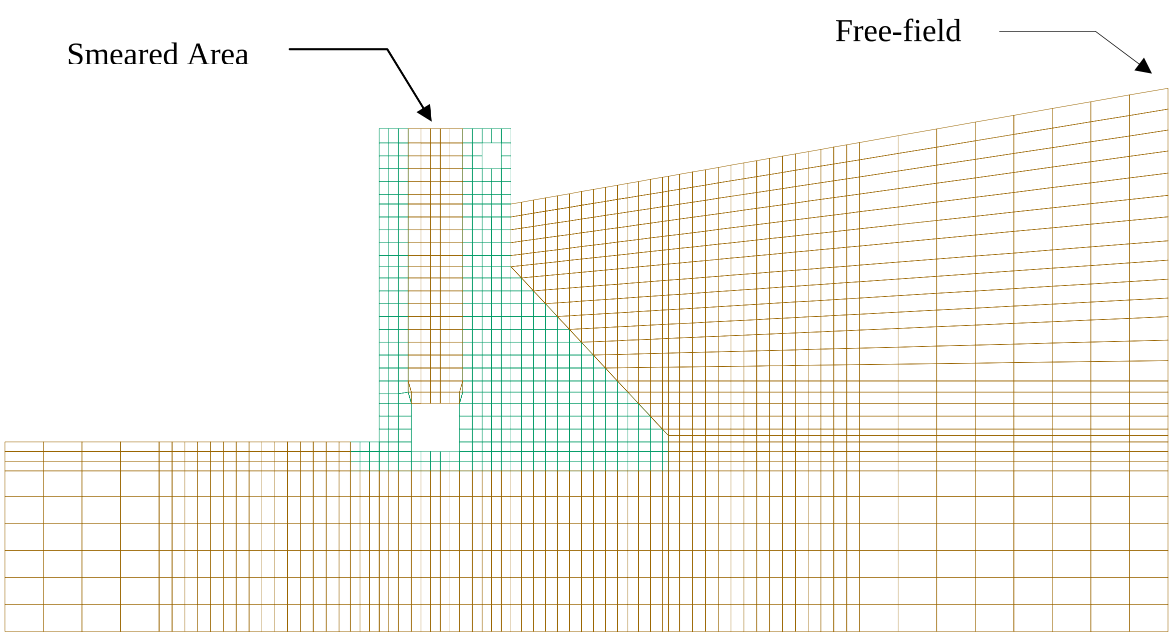

Figure G-4. Finite-element mesh for lock monolith, foundation rock and backfill soil

b. Strain-dependent Shear Modulus and Damping. The strain-dependent soil stiffness (shear modulus) and energy absorption (damping) characteristics were obtained from those available in the literature. For SSI analysis, a set of modulus reduction and damping curves based on data for similar soils (sand backfill and rock, Seed and Idriss 1970) were selected and is shown in Figures G-5 and G-6. In these Figures, G is the soil shear modulus and G_{max} is the soil shear modulus at low shear strain (strain less than 10^{-4} percent).

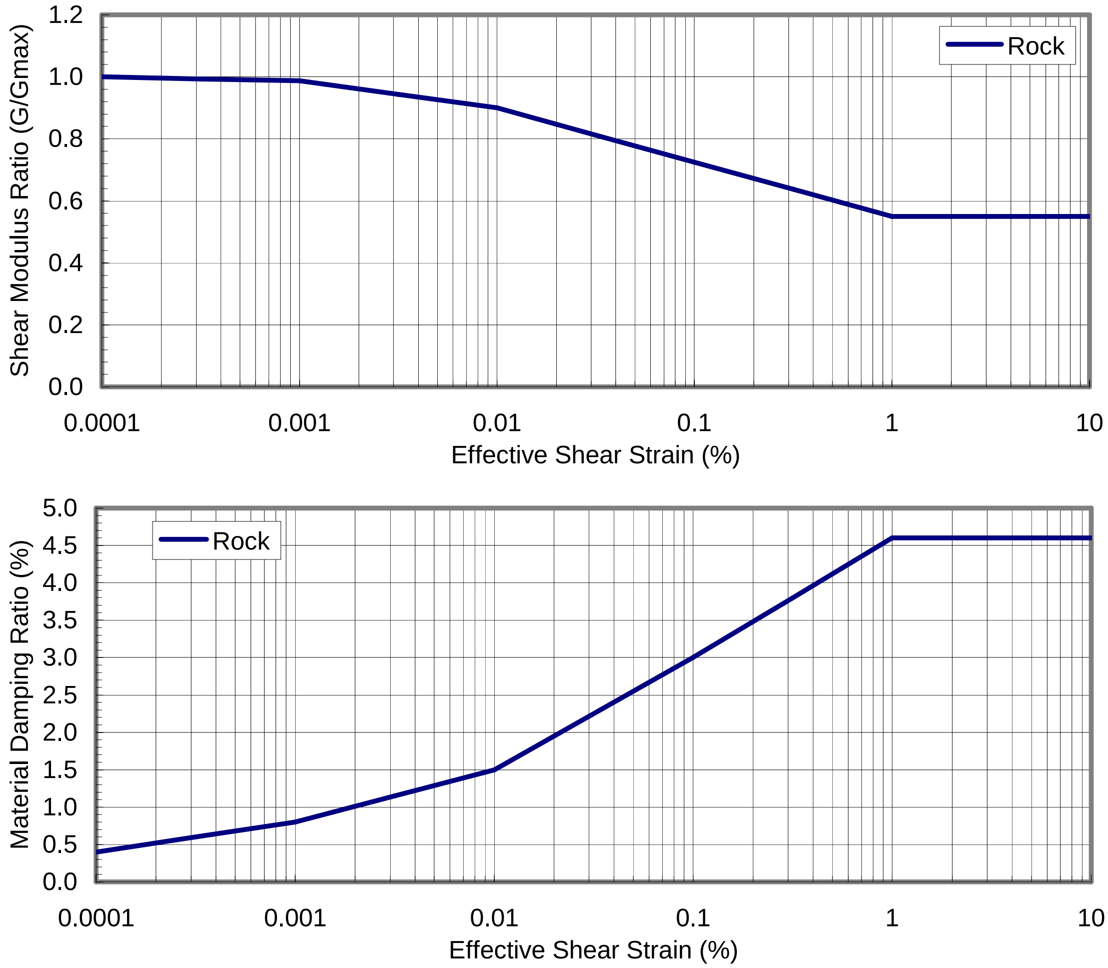

Figure G-5. Strain dependent material properties for rock

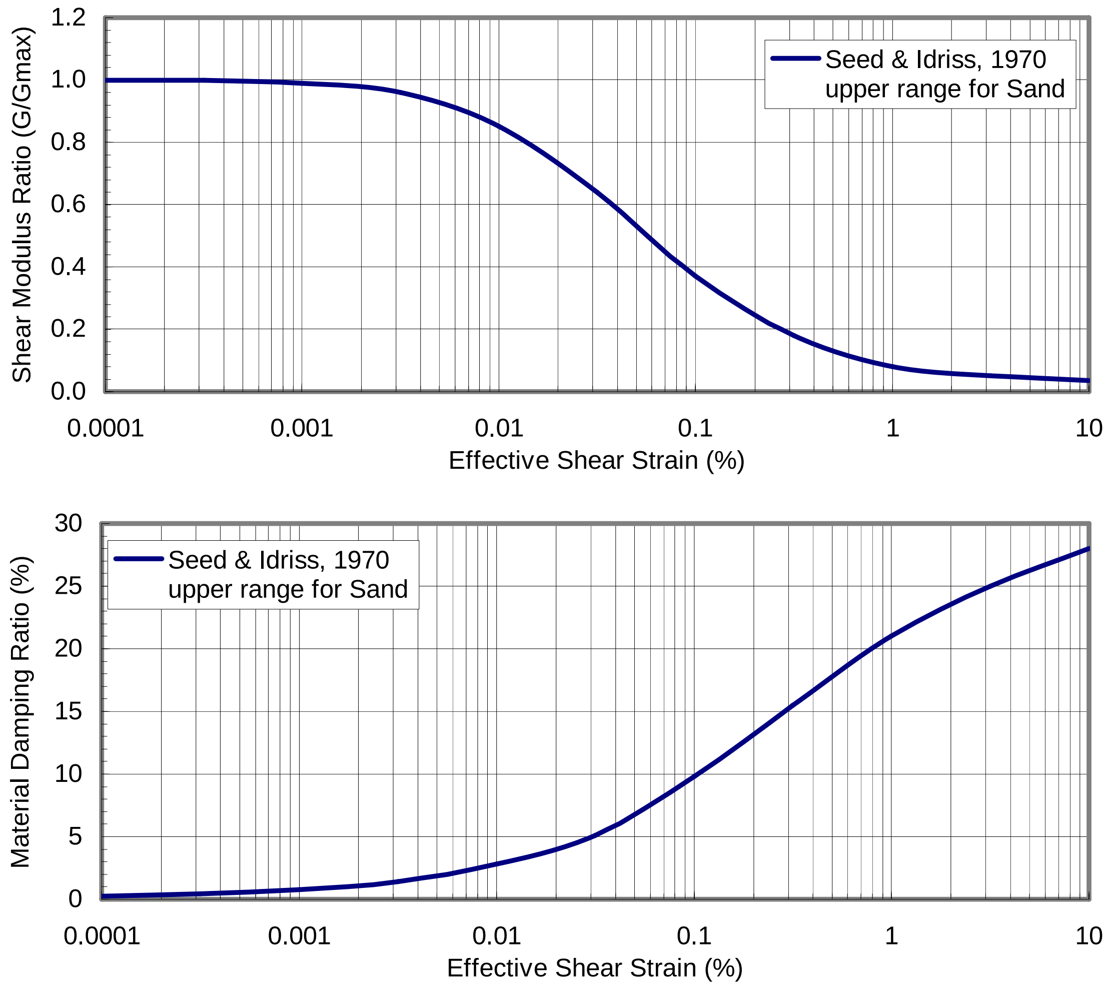

Figure G-6. Strain dependent material properties for sand

G-7. Loading Conditions

a. Static Loads. The static loads for the normal operating condition consisted of the dead weight and normal water pressures. Stress and deformation response due to static load cases were computed using the computer program SAP2000. The SAP2000 results were later converted to the QFLUSH model for superposition with the results of dynamic SSI analysis. The static and dynamic finite-element models, therefore, were identical in terms of geometry, mesh, and element types. The water pool elevation was set at El. 109.42 m (359 ft).

b. Earthquake ground motions. Dynamic SSI analyses for Kentucky lock wall were performed for the MDE level excitations using three input acceleration time histories. The peak ground acceleration for the MDE event was estimated to be 0.25g. The input earthquake acceleration time histories were obtained from a report prepared for the project (“Kentucky Lock Addition – Seismic Design Criteria, February 2001”). The selected earthquake records scaled to a peak ground acceleration of 0.25g for this example included the following:

1. MDE1 - 1989 Loma Prieta Earthquake: Anderson Dam Record, Far Field, M8.1.
2. MDE2 - 1985 Mexico City Earthquake: Papanoa Record, Far Field, M7.1
3. MDE3 – 1987 Superstition Hills Earthquake: Wildlife Record, Near Field, M5.8.

c. These records were selected from a set of 8 time-history records based on their duration of sustained strong motion and time steps. Only records with time steps equal to or less than 0.02 seconds with a Nyquist frequency of 25 Hz and higher were considered appropriate since records with long time steps lack energy in the high frequency range. Anderson and Papanoa records were selected because their "bracketed duration" of strong shaking was the largest. Wildlife record was selected from the near-field records again based on its longest bracketed duration of the strong shaking. A bracketed duration is defined as the time interval between the first and last acceleration peaks that are equal to or greater than 0.05g. The horizontal and vertical components of the selected acceleration records with their respective FFT are displayed in Figures G-7 to G-9.

d. Hydrodynamic force. Hydrodynamic forces were obtained from the inertia forces generated by the added masses attached to the concrete nodal masses. The water pool elevation for earthquake loading was set at 109.42 m (359 ft).

G-8. Presentation and Evaluation of Results

a. Free-Field Site Response. The first step in QFLUSH analysis is computation of the free field motions. In this example this was accomplished by using a column of elements at the right lateral boundary as the soil column, as shown in Figure G-4. Soil profile for the free-field computation consisted of uniform granular soil underlain by uniform rock whose material properties are given in Tables G-2 and G-3 and also in Figures G-5 and G-6. Variations of free-field peak horizontal acceleration with depth were obtained from the free-field site response analysis. They are shown in Figure G-10 for the horizontal and vertical components of each selected earthquake input. The results show that the ground motion changes very little within the foundation rock model. Consequently the ground motions recorded at the ground surface were directly applied at the base of the finite-element model. However, as the ground motion propagates upward, it is modified significantly by the backfill soil. Figure G-10 shows that the horizontal peak ground acceleration at the top of the backfill soil is about 0.63g for Anderson, 0.48g for Papanoa, and 0.56g for the Wildlife record, which has amplified by factors of 2.52, 1.92, and 2.24 over the peak bedrock acceleration. Varying amplification factors for the records are not surprising due to their varied response spectrum characteristics shown in Figure G-11.

b. Nonlinear behavior of Backfill Soil. In the equivalent-linear approach (QFLUSH), the soil behavior is specified as shown in Figure G-6, where the shear modulus and damping ratio vary with the shear strain amplitude. The values of shear modulus and damping ratio are determined by iterations so that they become consistent with the level of strain induced in each soil layer. Figure G-12a compares the initial shear-wave velocity with the final strain-compatible shear-wave velocity as a measure of the level of nonlinear behavior. This figure shows that the shear-wave velocity decreases 40 to 60 percent from the top to bottom of the backfill soil as a result of soil softening. Figures G-12b and c indicates damping ratios as high as 23% for the horizontal and 14% for the vertical component of ground motions are achieved as the soil softens and strain amplitudes increase. Overall the level of nonlinear behavior is considered moderate.

c. Stress Results. The QFLUSH post-processor, QFPOST, provides time-history plots of 2D element stresses, contour plots of maximum and minimum element stresses, and snap shots of element stresses at any user defined time steps. Figure G-13 is an example of stress time histories for four concrete elements located at the toe of the wall. The time-history plots include horizontal, vertical, and shear stresses for all four elements. Using stress time histories for all elements, the post-processor searches for the maximum, minimum, and snap shots at any given time to prepare contour plots such as those shown in Figures G-14 to G-16 for Anderson earthquake record. Figure G-14 represents envelopes of maxim vertical stresses for the concrete, rock, and backfill soil. The positive values indicate tensile stresses and negative values compressive stresses. Note that tensile stresses of 0.275 MPa (40 psi) at the heel of the lock wall are relatively small. Figure G-15 displays a snap shot of horizontal normal stresses at the time of 15.83 seconds which coincides with a peak tensile horizontal stress. Overall the stress magnitudes are moderate. As shown in this figure, the maximum tensile stress of 0.345 MPa (50 psi) occurs at the top of the backfill soil near the lock wall. Figure G-16 is another snap shot showing shear stresses at the time of 15.83 seconds. This figure shows a maximum shear stress of about 0.310 MPa (45 psi).

d. Section Forces and Moments. The stress results can be used to compute section forces and moments to assess sliding and rotational stability of the lock wall. This is facilitated by QFPOST capabilities, which provides time histories of resultant axial forces, shear forces, and moments at user defined sections. Figure G-17 shows three horizontal Sections HS1, HS2, and HS3 that may need to be checked against sliding. For this example time histories of resultant forces and moments at Section HS1 are provided in Figures G-18 to G-20 for all three selected earthquake records. Each figure includes time histories of the normal and shear forces with the moments. The shear forces in these figures represent the shear demands, and the normal forces in conjunction with a friction angle, and cohesion if applicable, can be used to compute the shear resistance for that section.

e. Instantaneous Sliding Factors of Safety. Knowing the shear demands and capacities (i.e. resistance), the instantaneous factor of safety for the section can be computed from the ratio of shear demands to shear capacities and plotted as a time history. In this example a conservative friction angle of 35 degrees with zero cohesion was used. The results show that for Section HS1 the instantaneous factors of safety vary between 3 and 11 during the ground shaking (bottom graphs in Figure G-18 to G-20). The lock wall therefore has ample factor of safety against the sliding. The moment demands can be used similarly and compared with the restoring moment to assess the rotational stability condition.

f. Dynamic Backfill Soil Pressure. Dynamic soil pressure is another parameter of interest that can be obtained from the SSI analysis. In this example two vertical sections VP1 and VP2 were selected for this purpose (Figure G-17). Section VP1 is located at the toe of the wall and VP2 at some distance away so it is less affected by the motion of the wall. The backfill soil pressures (i.e. normal horizontal stresses) along VP1 and VP2 were obtained at several instants of peak responses and are displayed in Figures G-21 to G-23 for all three earthquake ground motions. Note that the smooth pressure distributions on these graphs belong to VP2 and those appearing jagged at lower elevations to VP1. The jagged nature of the pressure distributions for VP1 is attributed to toe motions of the wall. Overall, soil pressures at VP1 and VP2 are similar but the shape of the pressure distribution varies with time and the earthquake ground motion. Pressure distributions for Anderson (Figure G-21) and Wildlife records (Figure G-23) are quite similar, but they differ with those for Papanoa. This observation shows that the dynamic soil pressure changes during the excitation and that it is affected by characteristics of the ground motion. This finding indicates that the simplified dynamic soil pressure should be used with caution.

G-9. Conclusions

An example of the time-history dynamic soil-structure-interaction analysis for a lock gravity wall with backfill soil was illustrated. The procedure was used to analyze the seismic response of the Culvert Valve Monolith L4 of the Kentucky Lock Addition under the MDE loading conditions. Three different earthquake acceleration time histories were used to account for the variability of ground motion characteristics. Modeling aspects of the SSI analysis was discussed and the use of time-history analysis results to access stability condition of the lock wall was described. This was accomplished by computing resultant normal and shear forces along selected sections, and then using them to compute instantaneous factors of safety against the sliding. The resulting instantaneous or time-history of factors of safety indicated ample margin of safety against sliding. The dynamic soil pressures at two vertical sections within the backfill were also retrieved to determine general distribution shapes and dependence on characteristics of the ground motion. The results show that the simplified dynamic soil pressures used in practice differ significantly from those obtained in this example. Therefore, in situations where the backfill soil plays an important role on the seismic response of the structure, the SSI method of analysis is recommended.

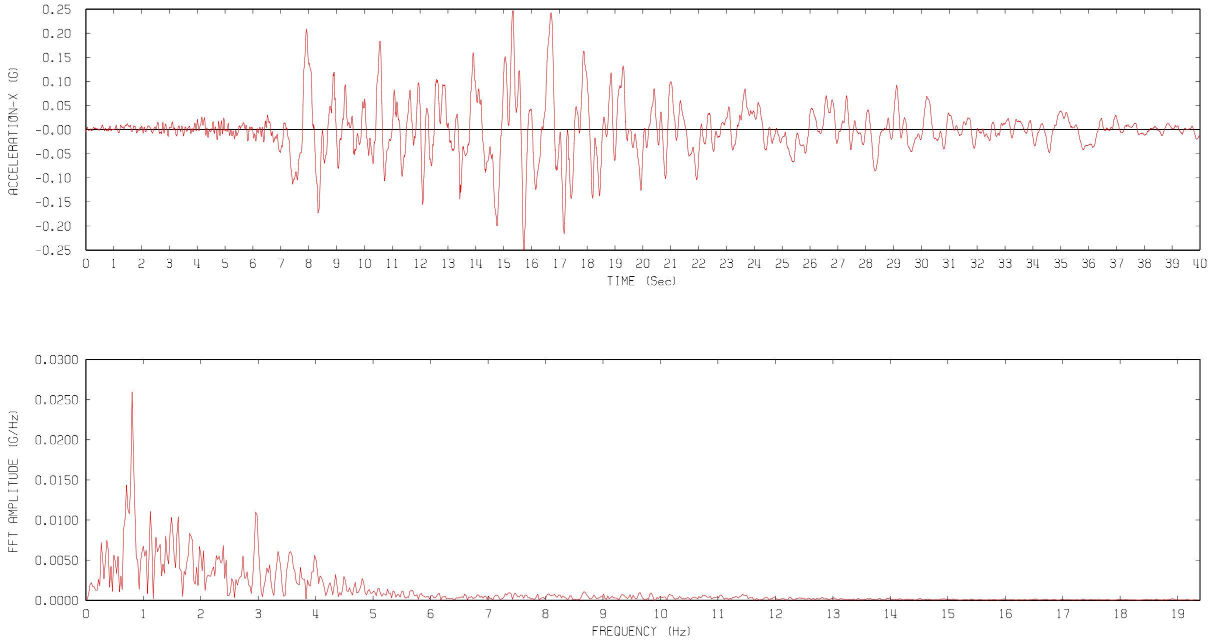

(a) Horizontal component

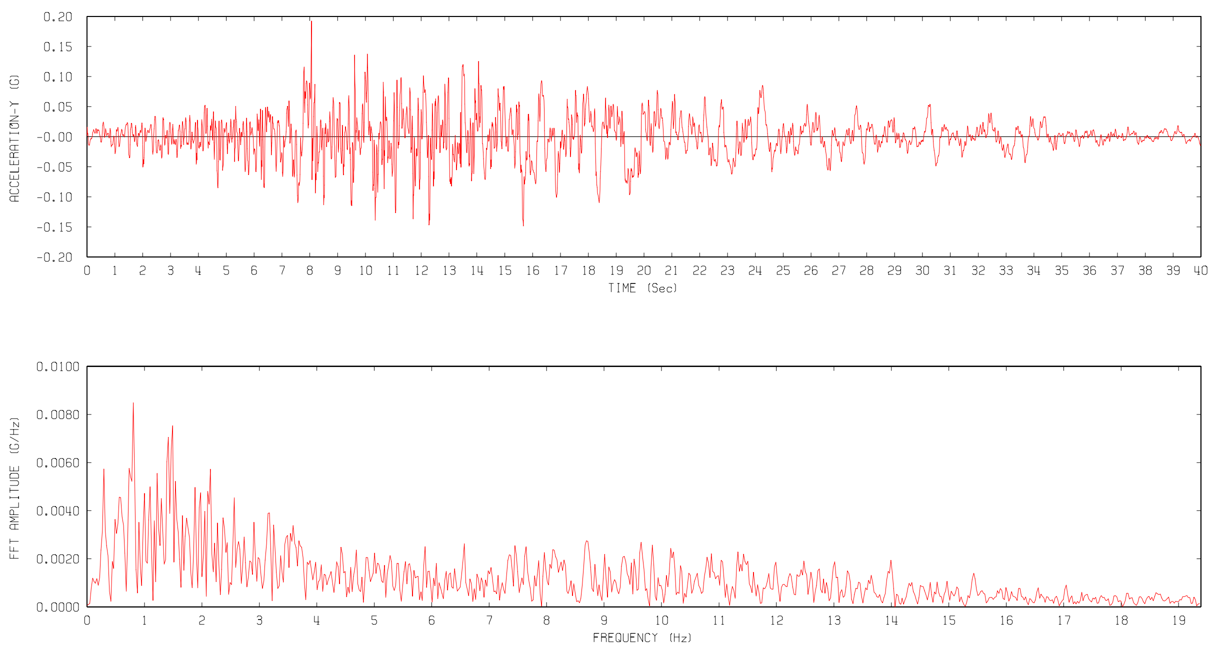

(b) Vertical component

Figure G-7. Time history and FFT of Anderson Dam acceleration record

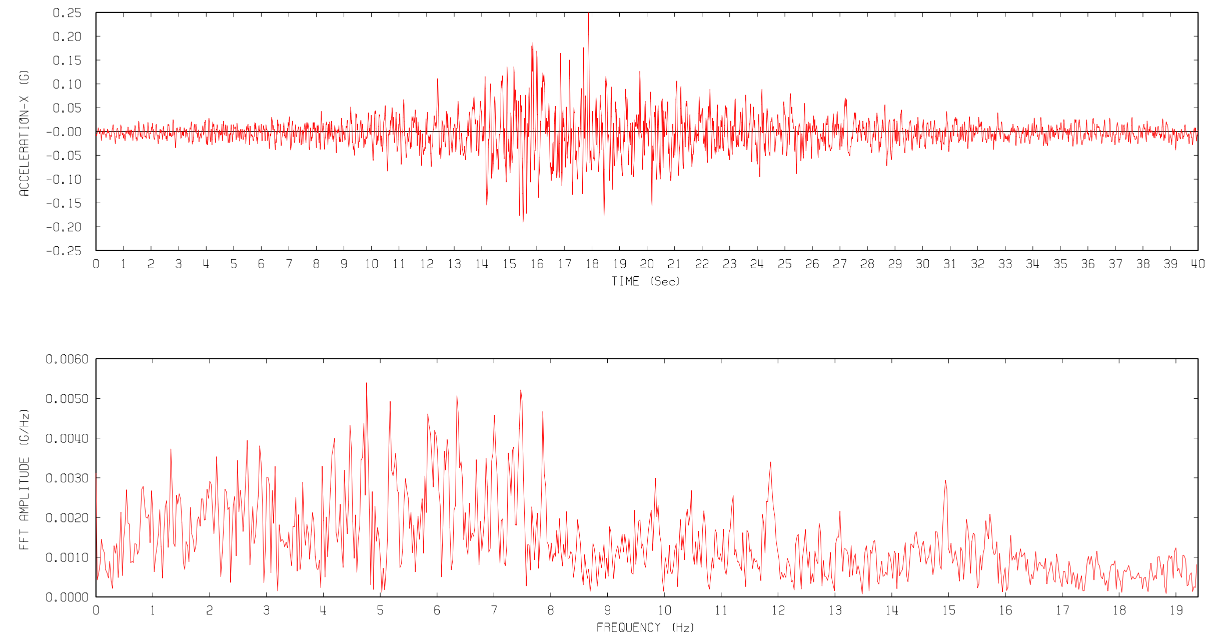

(a) Horizontal component

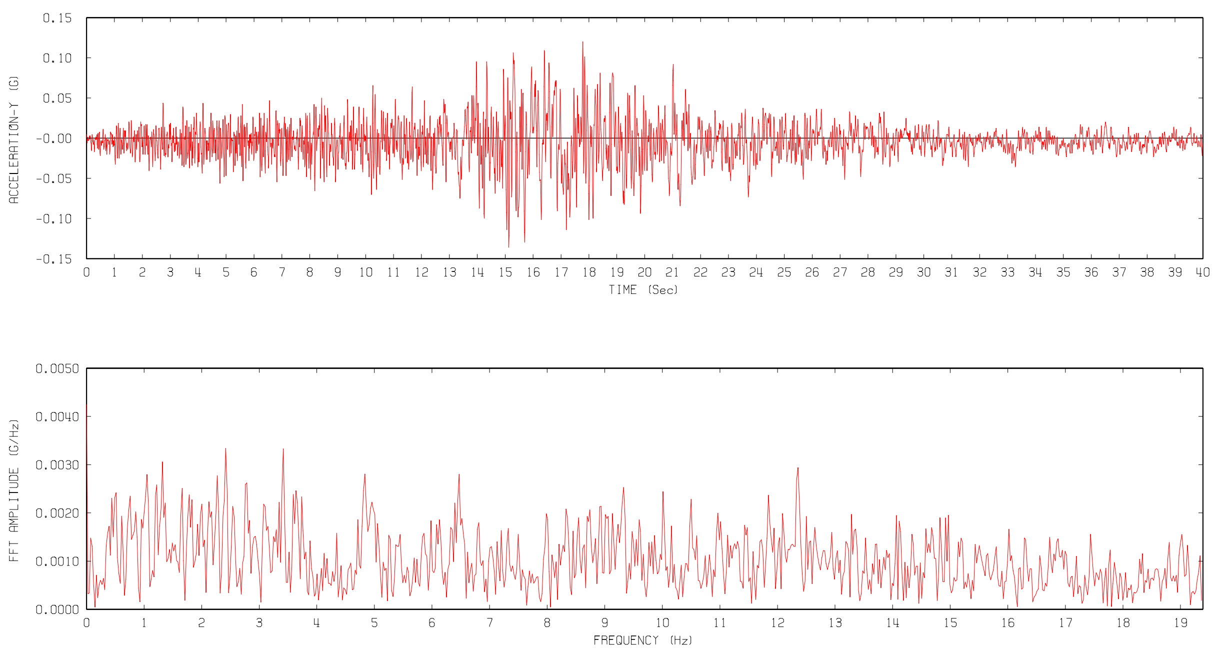

(b) Vertical component

Figure G-8. Time history and FFT of Papanoa acceleration record

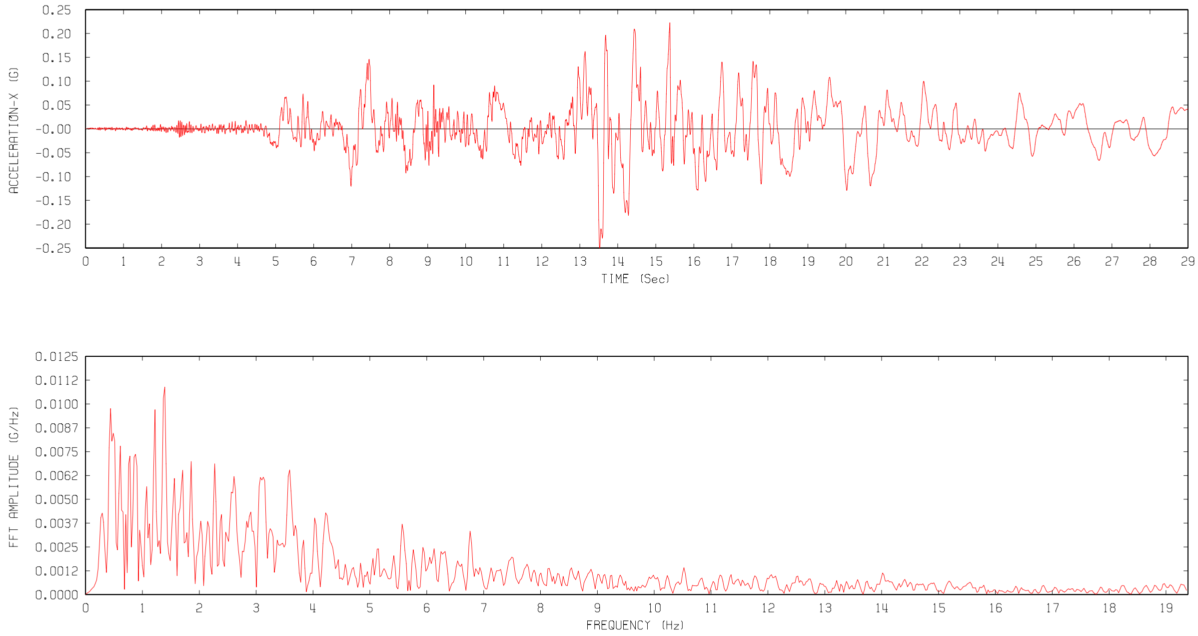

(a) Horizontal component

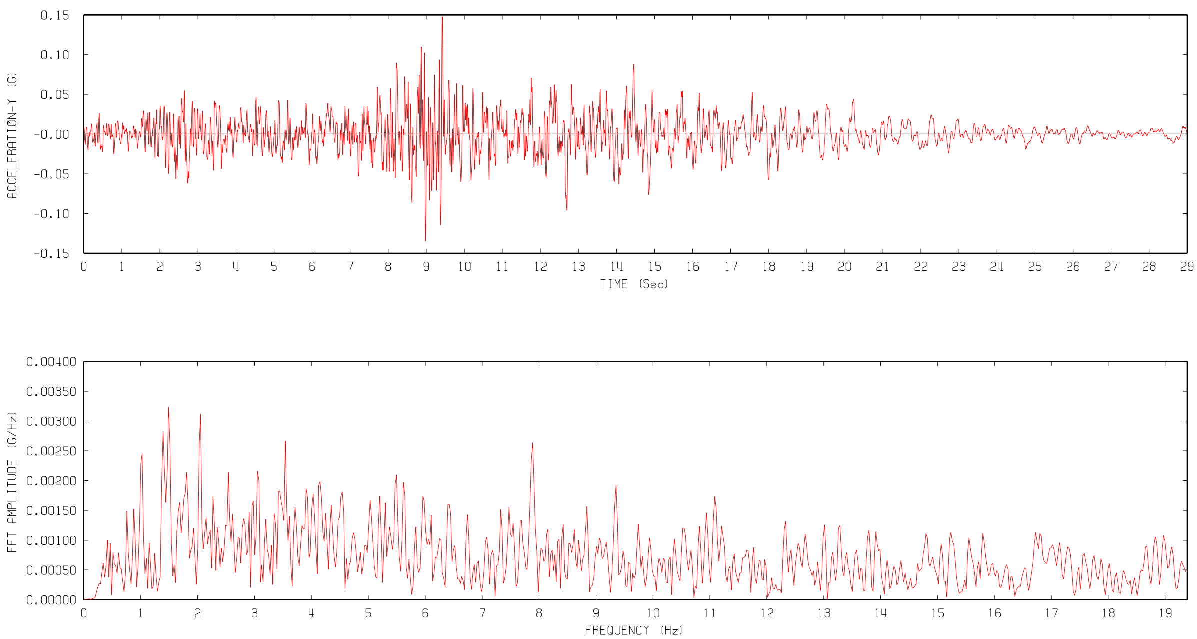

(b) Vertical compoenent

Figure G-9. Time history and FFT of Wildlife acceleration record

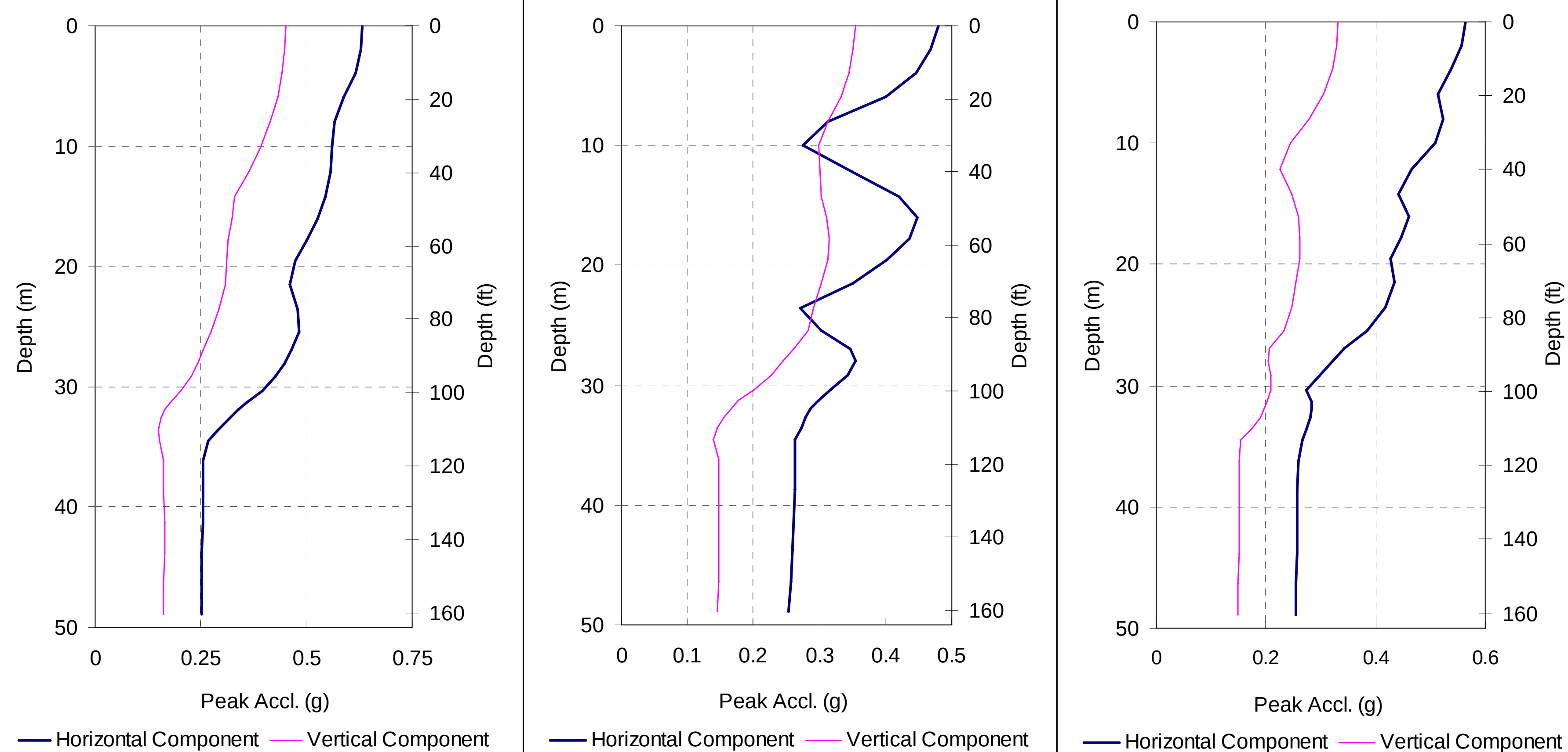

(a) Anderson ground motion | (b) Papanoa ground motion | (c) Wildlife ground motion

Figure G-10. Variation of peak acceleration with depth

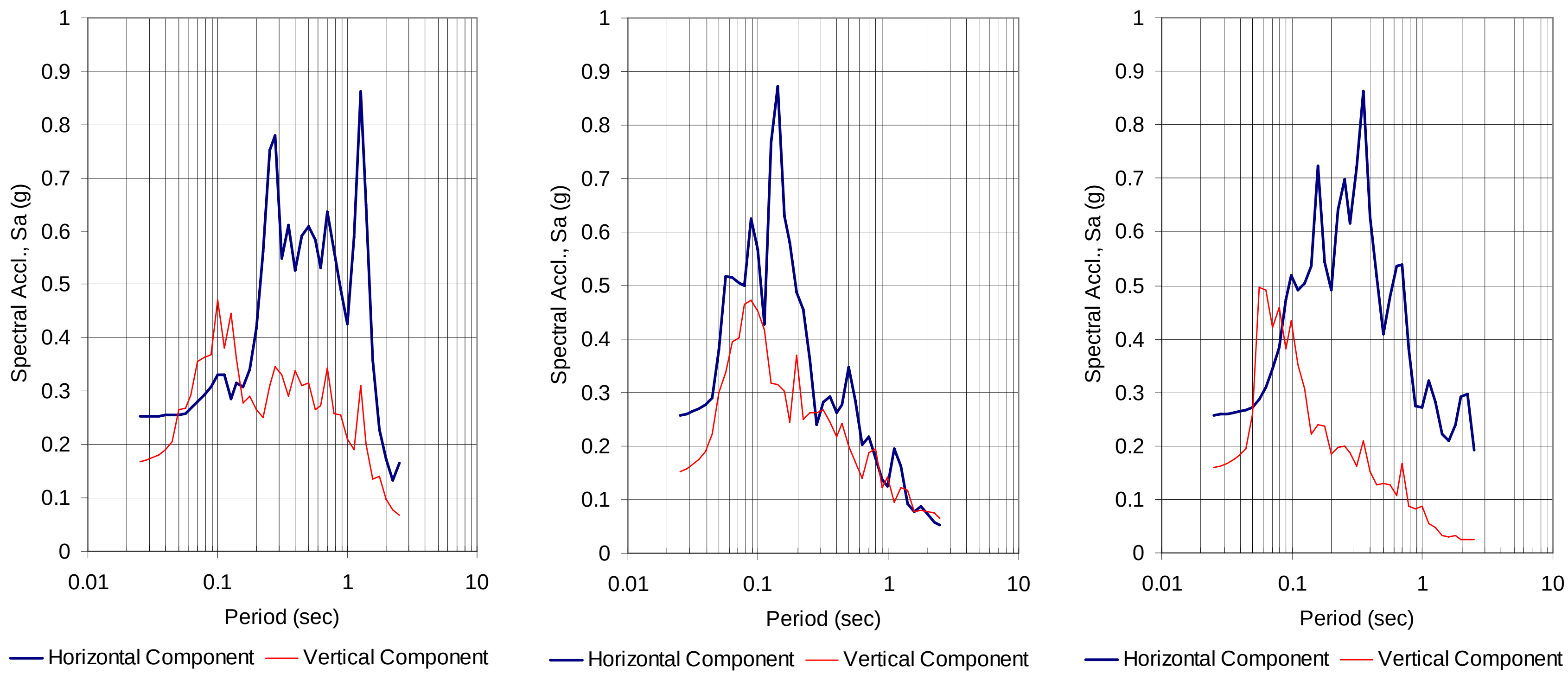

(a) Anderson ground motion (b) Papanoa ground motion (c) Wildlife ground motion

Figure G-11. Rock motion response spectra (5% damping)

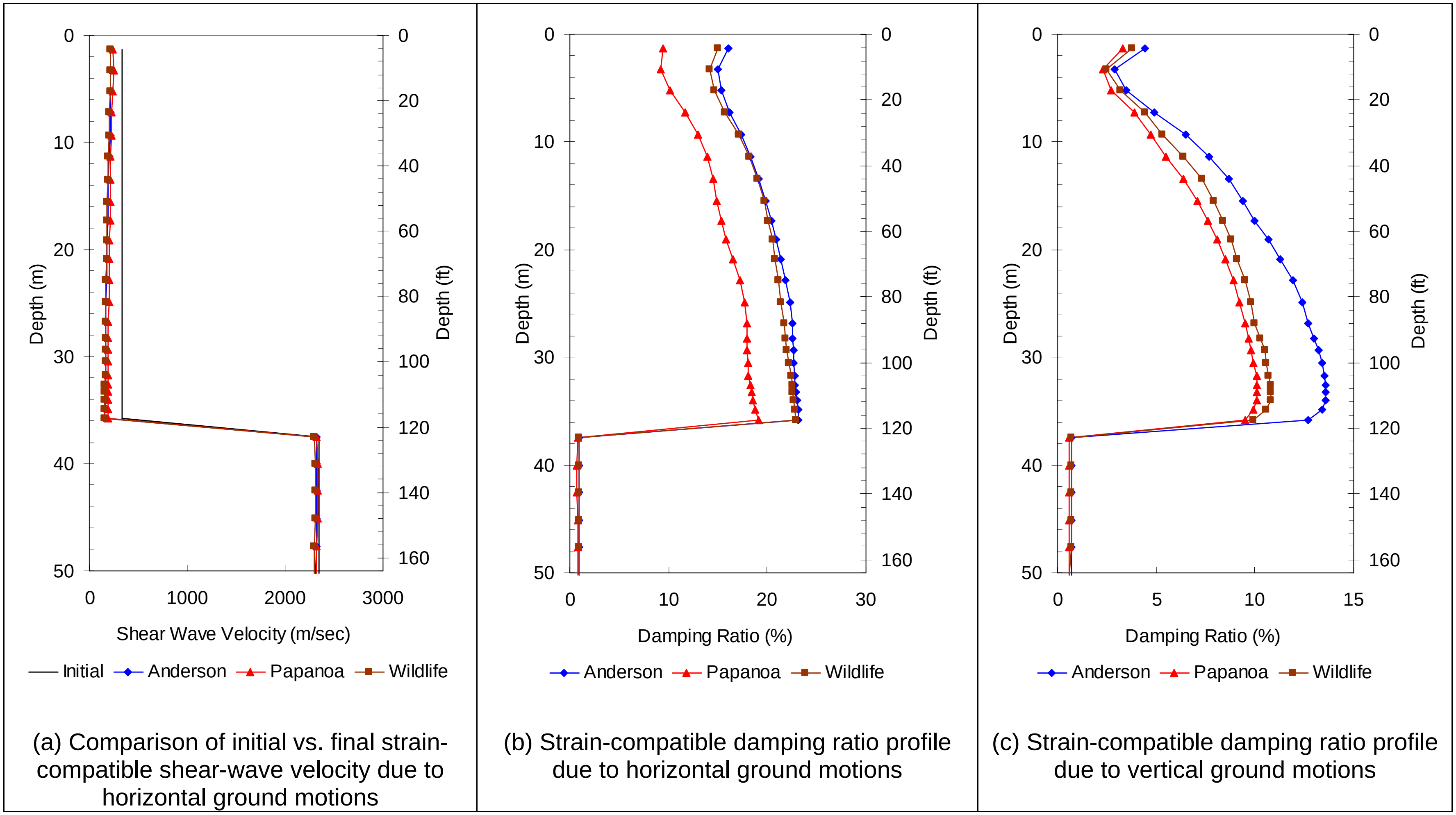

Figure G-12. Final strain-compatible shear-wave velocity and damping ratio profiles

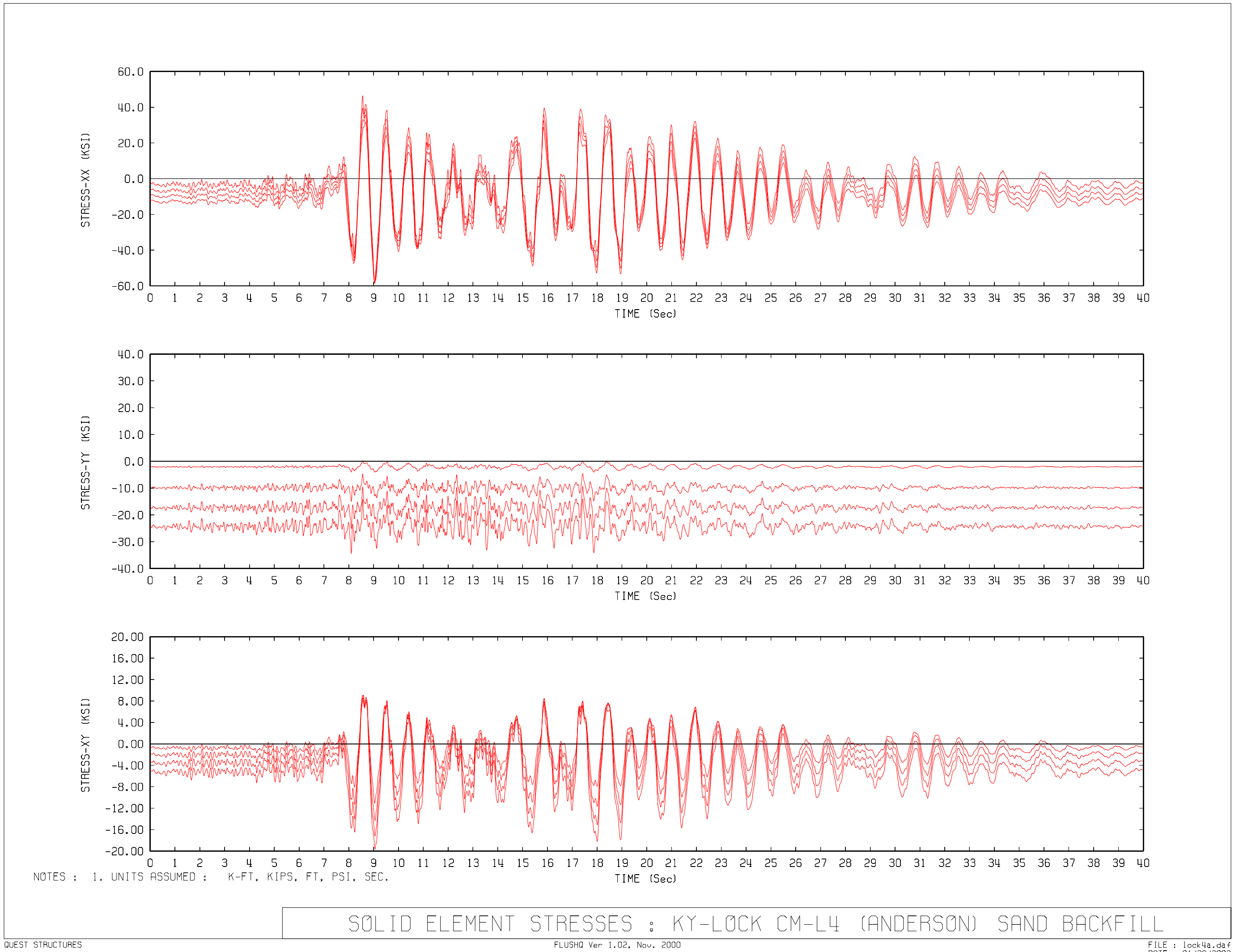

Figure G-13. Time history of horizontal (σ_{xx}), vertical (σ_{yy}), and shear (σ_{xy}) stresses for four elements at the toe of lock wall

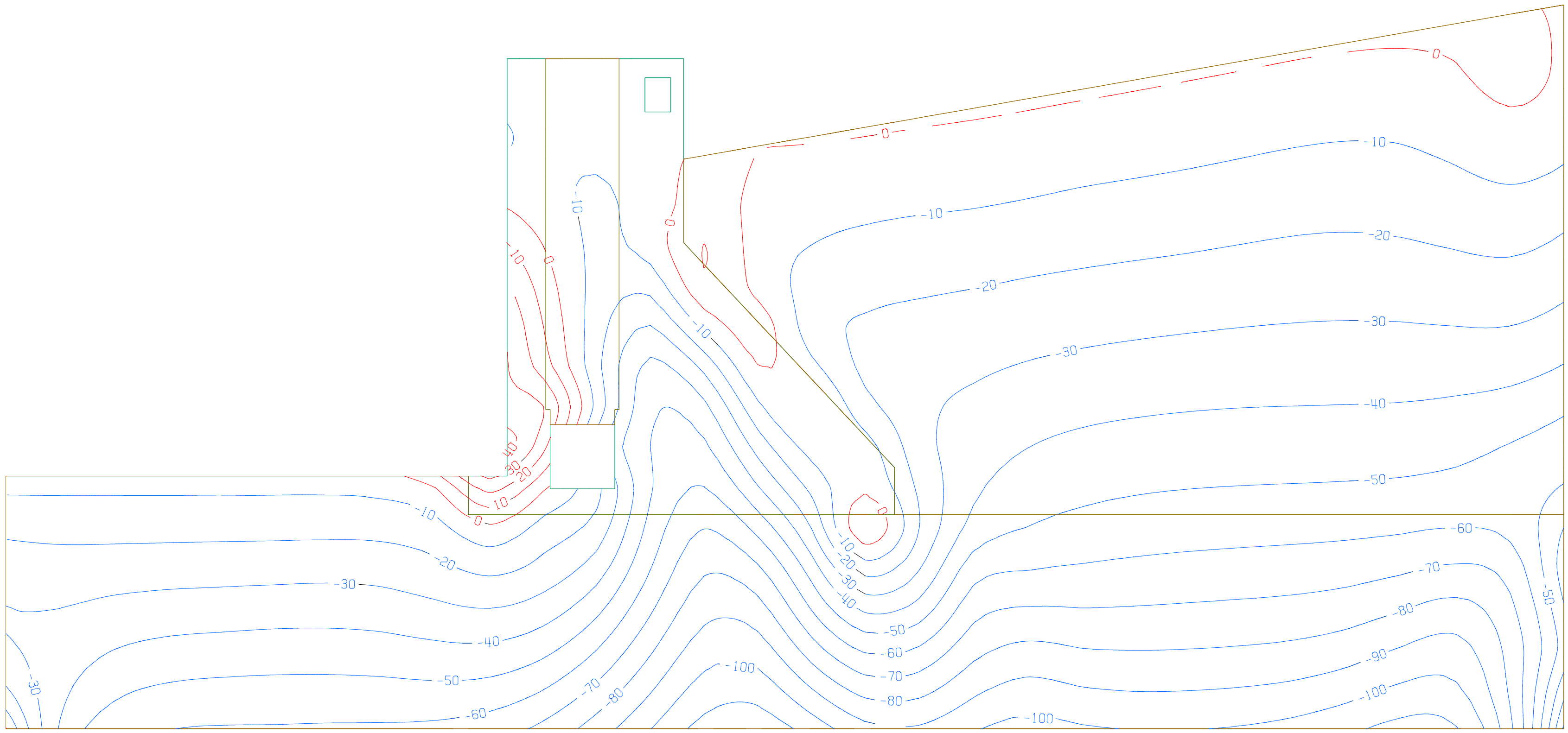

Figure G-14. Maximum vertical stress contours for Anderson earthquake record

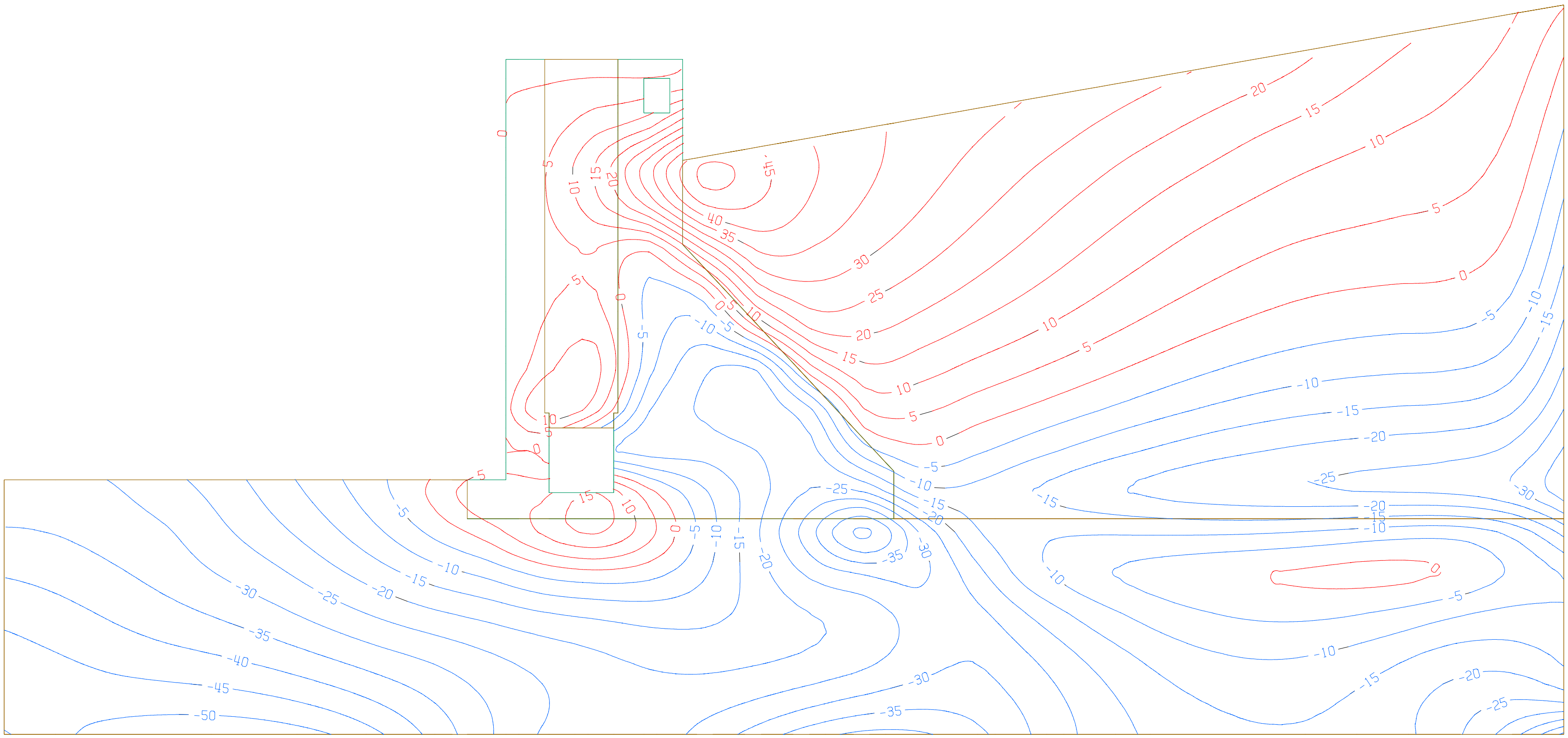

Figure G-15. Snap shot of horizontal stresses at t = 15.83 sec. for Anderson earthquake record

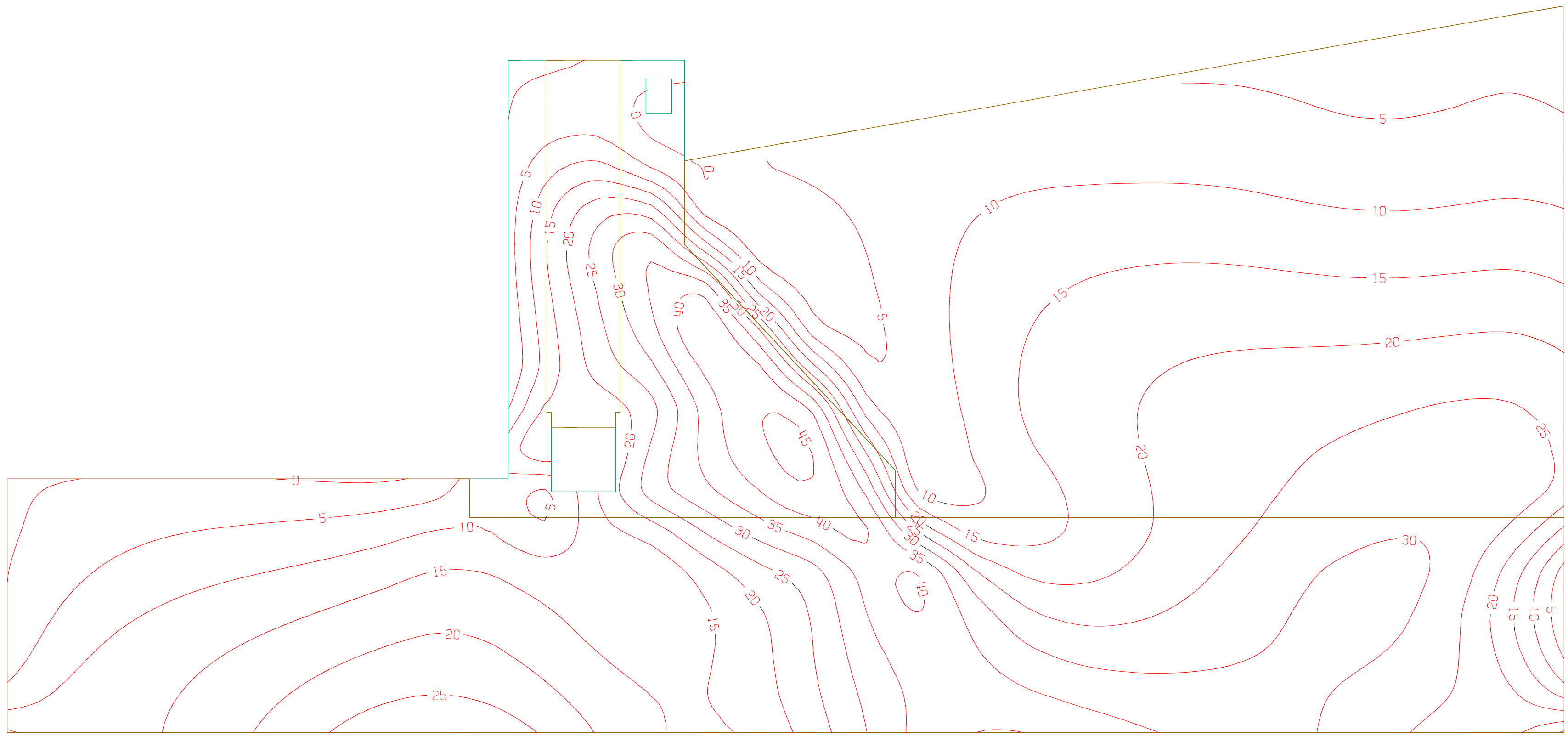

Figure G-16. Snap shot of shear stresses at t = 15.83 sec. for Anderson earthquake record

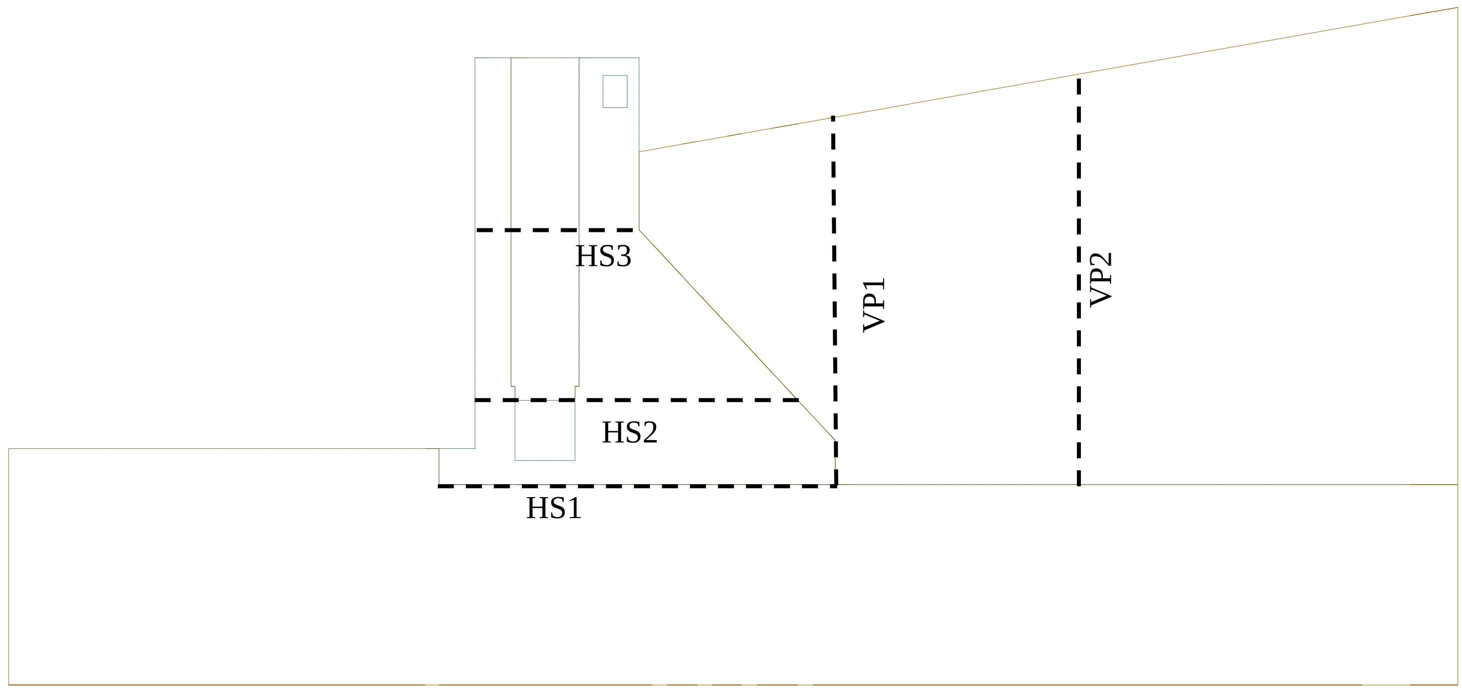

Figure G-17. Horizontal and vertical sections used in the analysis

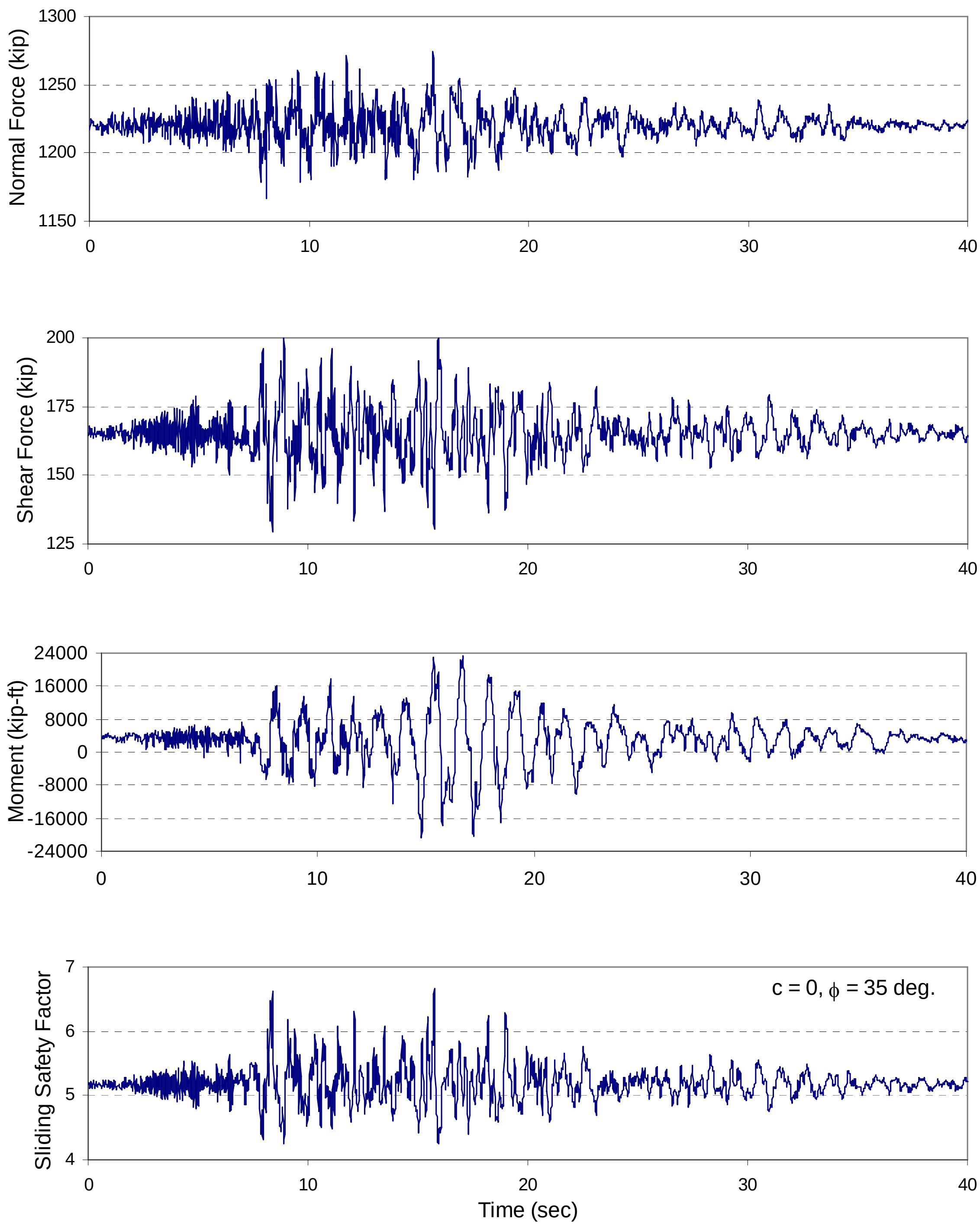

Figure G-18. Time histories of normal force, shear force, moment, and sliding safety factor at Section HS1 for Anderson earthquake record

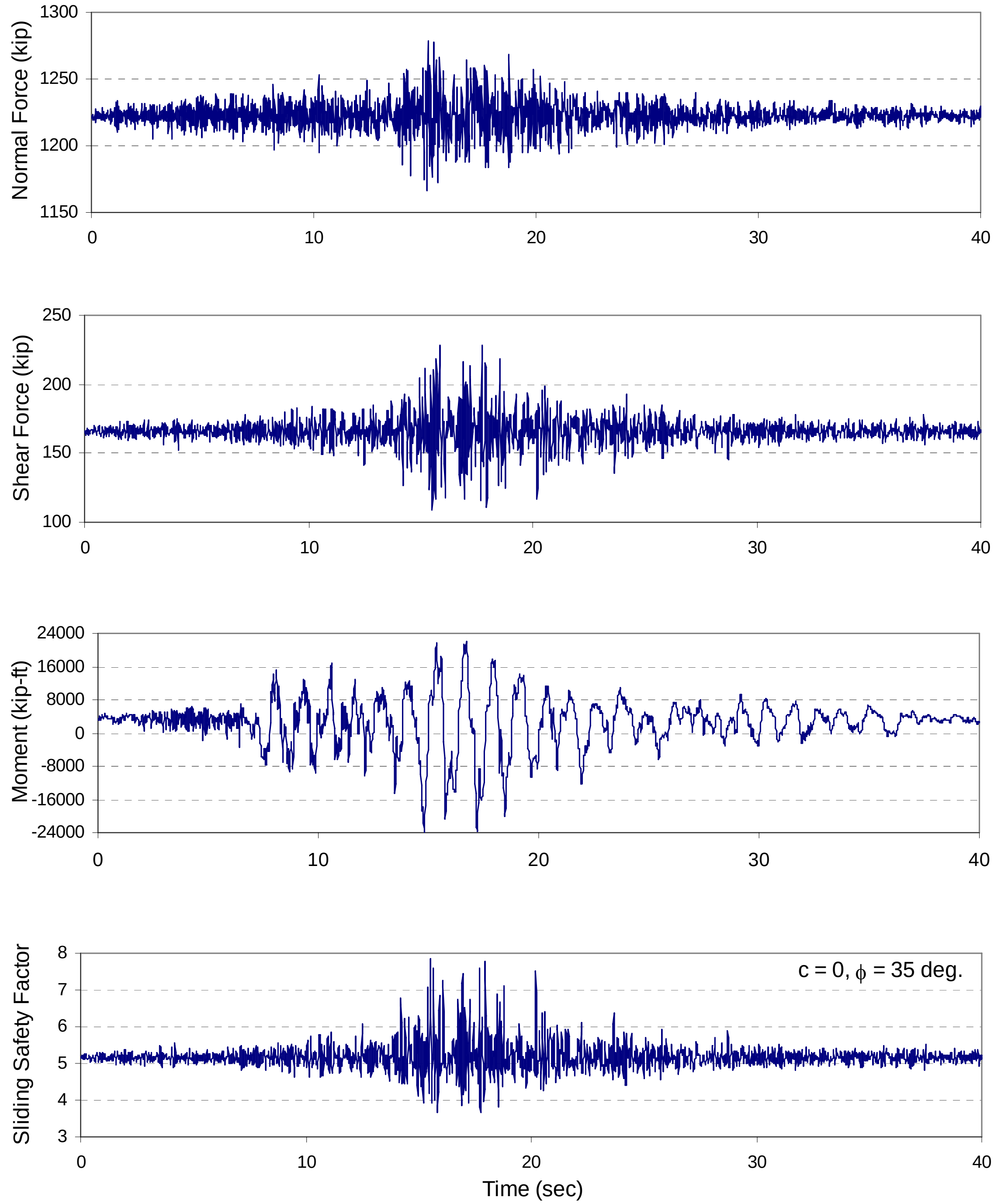

Figure G-19. Time histories of normal force, shear force, moment, and sliding safety factor at Section HS1 for Papanoa earthquake record

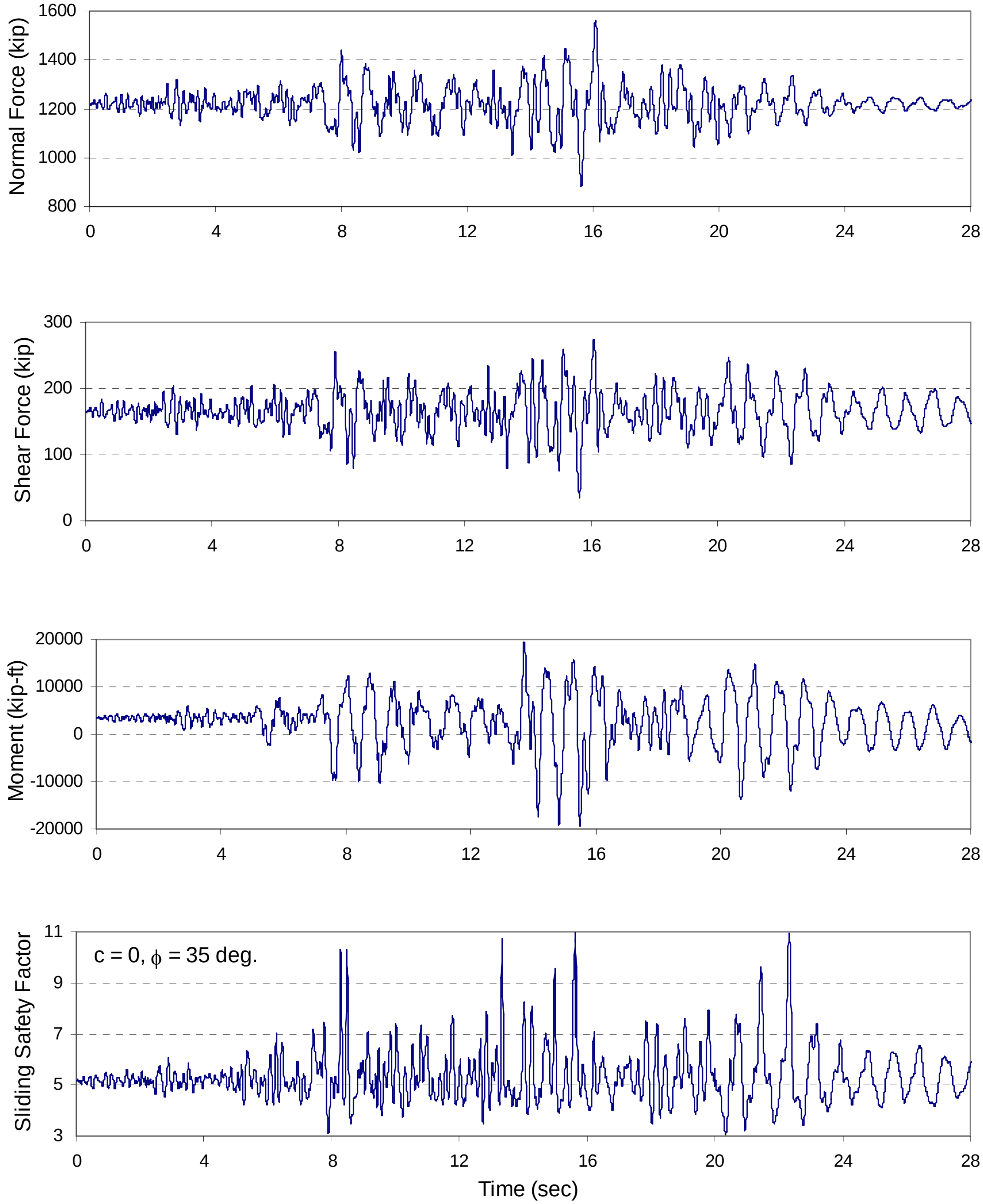

Figure G-20. Time histories of normal force, shear force, moment, and sliding safety factor at Section HS1 for Wildlife earthquake record

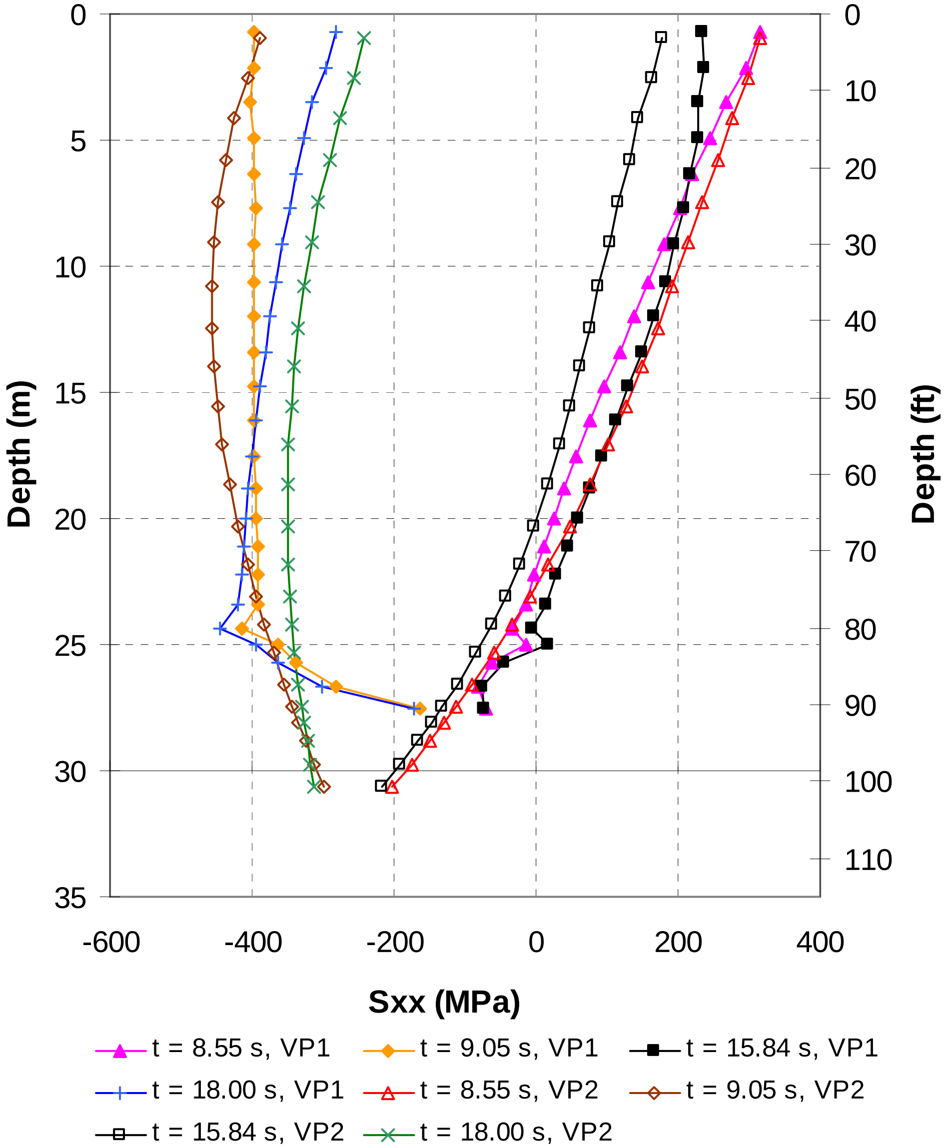

1 MPa = 145 psi

Figure G-21. Dynamic soil pressure profiles (normal stress Sxx) along vertical planes VP1 and VP2 at different instants of peak responses (Anderson ground motion)

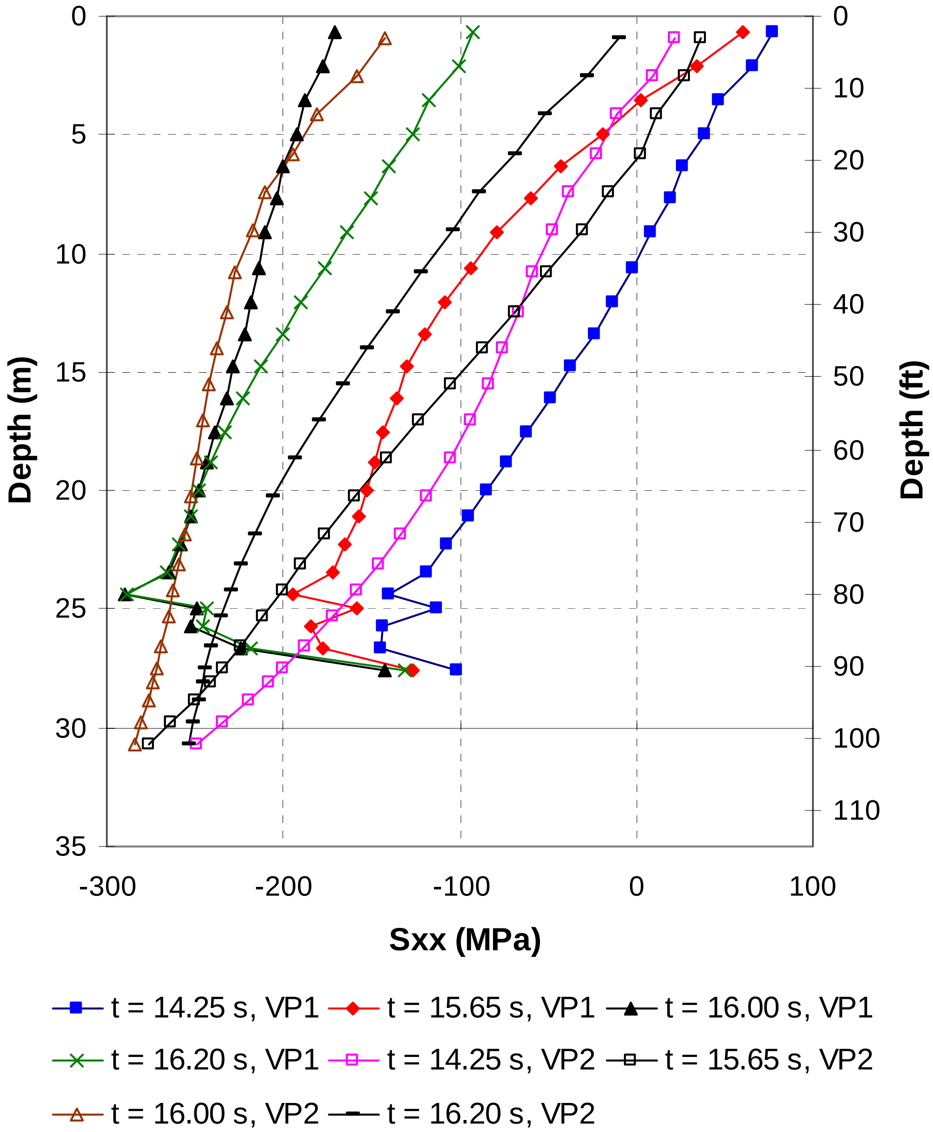

1 MPa = 145 psi

Figure G-22. Dynamic soil pressure profiles (normal stress, Sxx) along vertical planes VP1 and VP2 at different instants of peak responses (Papanoa ground motion)

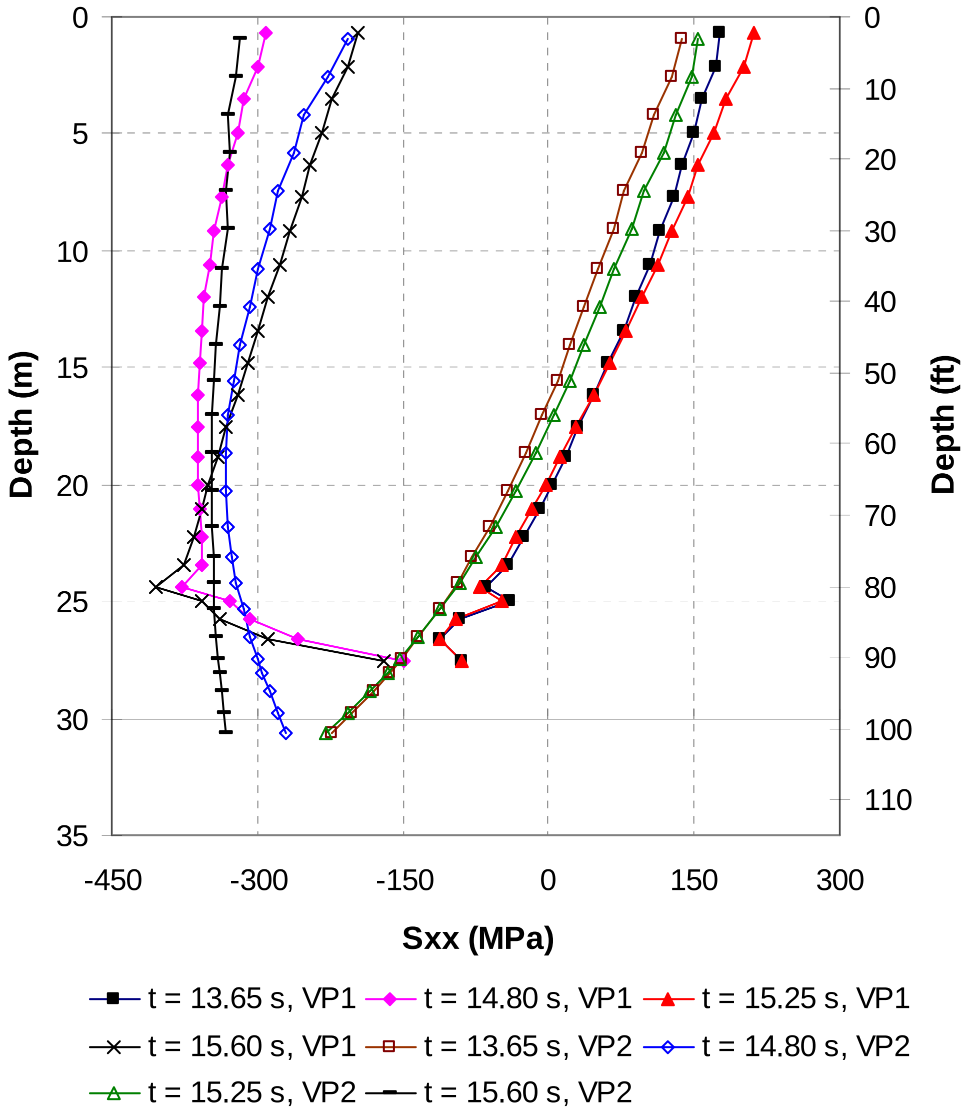

1 MPa = 145 psi

Figure G-23. Dynamic soil pressure profiles (normal stress, Sxx) along vertical planes VP1 and VP2 at different instants of peak responses (Wildlife ground motion)